East European Journal of Physics. 4. 291-297 (2025)
DOI:10.26565/2312-4334-2025-4-27 ISSN 2312-4334

ENHANCING AND OPTIMIZING OPTICAL PROPERTIES OF BIFACIAL SOLAR CELLS BY INCORPORATING METAL NANOPARTICLES

Murodjon M. Komilov[1], Rayimjon Aliev[1], Avazbek A. Mirzaalimov[2], Suhrob R. Aliev[4], Murodjon K. Abduvohidov[3], Navruzbek A. Mirzaalimov[1]*, J. Ziyoitdinov[1], Sodiqjon I. Temirov[1]

[1]*Andijan State University named after Z.M. Babur, 129, Universitet Str., 170100 Andijan, Uzbekistan*
[2]*Andijan State Pedagogical Institute, 4, Dostlik Str., 170100 Andijan, Uzbekistan*
[3]*Kokand University Andijan branch, 2-b, Bobursho Str., 170100 Andijan, Uzbekistan*
[4]*Andijan State Technical Institute, 56, Bobursho Str., 170100 Andijan, Uzbekistan*
**Corresponding Author e-mail: mirzaalimov90@mail.ru*
Received August 11, 2025; revised November 11, 2025; accepted November 15, 2025

In this study, the optical properties of a silicon-based bifacial solar cell with an n^+–p–p^+ structure were investigated using numerical simulation in the Sentaurus TCAD environment. Various metal nanoparticles were embedded in the emitter layer in a linear configuration to analyze their effects on light absorption and scattering. The study compared metal nanoparticles of platinum (Pt), gold (Au), silver (Ag), aluminum (Al), and copper (Cu). All nanoparticles were modeled with the same diameter (5 nm), and the current-voltage (I–V) characteristics were obtained for each configuration. The simulation results showed that platinum nanoparticles yielded the highest short-circuit current density of 13.8 mA/cm², while silver nanoparticles yielded the lowest, at 5.027 mA/cm². Optimal parameters were observed with nanoparticles of 5 nm in diameter. Furthermore, it was found that the photon absorption density for the most efficient metal type was 1.81 times greater than that of the reference structure without nanoparticles. Additionally, the spectral sensitivity of silicon shifted toward the ultraviolet region in the presence of metal nanoparticles. The study demonstrated enhanced utilization of the visible light spectrum, and due to the embedded nanoparticles, the overall absorption coefficient of the bifacial solar cell increased by a factor of 1.33, aligning more effectively with the visible spectral range.
Keywords: *Silicon; Metal nanoparticles; Bifacial solar cell; Sentaurus TCAD; Nanoplasmonic effect*
PACS: 85.60.Bt, 78.20.Bh, 84.60.Jt

INTRODUCTION

Among renewable energy sources, solar energy is gaining an increasingly important role in the global energy system. This form of energy is environmentally friendly and represents an inexhaustible energy source [1]. Enhancing the efficiency of solar cells is currently one of the key research directions in science and technology. In particular, bifacial solar cells, distinguished by their ability to absorb light from both the front and rear sides, can increase their overall energy generation potential by up to 10–30% [2].

Silicon-based solar cells belong to the class of devices that are highly sensitive to environmental conditions. The effects of light intensity [3], temperature [4], and the angle of light incidence on solar cell performance has been widely investigated. It has been established that an increase in temperature leads to a slight rise in short-circuit current, while the open-circuit voltage decreases significantly, resulting in an overall reduction of the power conversion efficiency [5]. Numerous comprehensive studies have been conducted to enhance the efficiency of solar cells and minimize losses. In general, there are three primary loss mechanisms in solar cells: thermal [6], electrical [7], and optical [8]. In conventional silicon-based solar cells, more than 30% of the incident light is reflected from the surface [9]. To reduce this reflection coefficient, various anti-reflective coatings [10] and surface texturing techniques [11] have been developed. The surfaces of silicon-based solar cells are commonly coated with SiNx or SiO_2, as these materials possess passivation properties and have refractive indices between those of air and silicon [12]. In practice, surface texturing is achieved using alkaline or acidic solutions, and silicon wafers with a (100) crystal orientation are typically employed [13]. Since the bandgap of silicon is 1.12 eV, it mainly absorbs photons in the visible spectral range. According to the quantum efficiency function, solar cell materials do not absorb photons with energies lower than the bandgap. If the photon energy is much greater than the bandgap, the excess energy is converted into hot electrons. These high-energy hot electrons quickly lose their excess energy through phonon emission, returning to the valence band and thus not contributing to the photocurrent. Therefore, to modify the absorption spectrum of solar cells, luminescent materials [14] or metallic nanoparticles [15] are often incorporated.

In converting solar energy into other forms, the device's optical properties play a crucial role. Surface texturing of various shapes on solar cells has been effectively employed to enhance light absorption [16]. Due to multiple refractions of sunlight at the surface, its energy is absorbed more efficiently. The presence of a p–n junction near the surface requires maximizing light absorption in its vicinity [17]. Increased light absorption close to the p–n junction results in a higher generation rate of charge carriers [18]. Therefore, surface textures with varying heights are fabricated on solar cells [19].

Cite as: M.M. Komilov, R. Alieva, A.A. Mirzaalimov, S.R. Aliev, M.K. Abduvohidov, N.A. Mirzaalimov, J. Ziyoitdinov, S.I. Temirov, East Eur. J. Phys. 4, 291 (2025), https://doi.org/10.26565/2312-4334-2025-4-27

These textures cause incident light rays to undergo multiple reflections within the structure, thereby increasing their interaction with the surface. Consequently, the degree of light absorption by the surface is significantly enhanced.

Currently, methods for generating additional charge carriers near the p–n junction are being continually improved. In particular, the use of metallic nanoparticles to enhance the optical and electrical properties of solar cells has emerged as a promising approach [20]. Metallic nanoparticles such as gold (Au), silver (Ag), and platinum (Pt) can enhance light scattering and absorption through the localized surface plasmon resonance (LSPR) phenomenon [21][22]. This effect leads to a localized enhancement of the electric field around the nanoparticles, thereby increasing the number of photons reaching the active layer [23]. Based on these mechanisms, numerous studies have confirmed that modifying solar cells with metallic nanoparticles can broaden the optical absorption spectrum, enhance scattering angles, and ultimately improve photogeneration efficiency [24][25]. For example, J. Zhu et al. demonstrated that the application of nanostructures could double the light absorption in illuminated solar cells**Error! Reference source not found.**.

In this study, the optical and electrical properties of bifacial silicon-based solar cells were investigated by introducing metallic nanoparticles (Au, Pt, Cu, Al, Ag) into the emitter layer through numerical modeling using the Sentaurus TCAD software package. Based on the simulation results, the effects of nanoparticle radius and material type on the photocurrent density and current–voltage characteristics were determined. The results showed that the optimal selection of nanoparticle parameters can significantly improve light absorption, thereby enhancing the overall efficiency of the solar cell.

MATERIALS AND METHODS

In this study, the effects of various metallic nanoparticles on the optical and electrical properties of a bifacial solar cell were investigated. The selected nanoparticles included silver (Ag), aluminum (Al), copper (Cu), gold (Au), and platinum (Pt). These materials were chosen due to their high nanoplasmonic activity as well as their strong light scattering and absorption capabilities, which play a crucial role in enhancing light–matter interactions within the solar cell. The device structure was based on a conventional n–p–p configuration, with both the front and rear sides designed to be light-absorbing. The top and bottom contacts consisted of metallic layers that efficiently received incident radiation through the intermediate layers. Metallic nanoparticles were embedded into the upper active emitter layer. In addition to the nanoparticle material, the radius (ranging from 1 to 25 nm) was considered as a variable parameter, and for each radius value, the optical and electrophysical characteristics of the solar cell were evaluated. During the optical simulations, the nanoparticle-specific surface plasmon resonance frequencies and absorption coefficients were taken into account. All numerical modeling procedures were performed using the Sentaurus TCAD software package.

During the simulation process, the following Sentaurus TCAD modules were employed as the primary tools:

SDE (Sentaurus Structure Editor) – used to design the geometric structure of the device, precisely defining the layers and positioning the nanoparticles;

SProcess – applied for adjusting dopant profiles and determining the exact placement of nanoparticles;

SDevice – used for electrophysical simulations of the device, including the calculation of current–voltage (I–V) and power–voltage (*P–V*) characteristics, electric field distribution, optical absorption levels, and photocurrent density;

Sentaurus Visual – employed for the visual analysis of the obtained results and for generating gradient maps of parameter distributions.

In the optical simulation stage, the complex absorption coefficients corresponding to each metallic nanoparticle were incorporated based on the optical models of the respective materials. The AM1.5G spectrum was adopted as the illumination source.

The primary photovoltaic parameters of the solar cell were determined using the current–voltage (I–V) characterization method, which enables the evaluation of output parameters for all types of solar cells. Fig. 1 presents the equivalent circuit of the device.

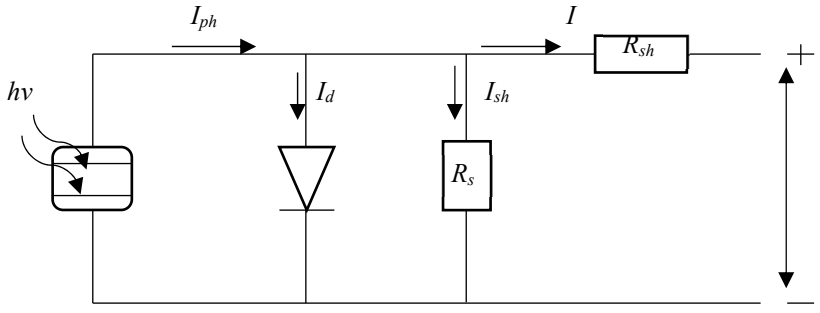

Figure 1. Equivalent circuit of a solar cell

Here, I_{ph} is the photocurrent, I is the total current in the circuit, I_d is the current flowing through the diode, and I_{sh} is the current passing through the shunt resistance. Applying Ohm's law to the entire circuit shown in Fig. 1, the total current can be expressed as:

$$I_{ph} = I + I_d + I_{sh} \tag{1}$$

The value of each current in the equation is determined separately. After that, the final working equation is obtained. The final equation can be seen in formula (2) below.

$$I_d = I_o\left[exp\left(\frac{U+IR_S}{nkT}q\right)-1\right],\ I_{sh}=\frac{U+IR_S}{R_{sh}}. \tag{2}$$

Here, I_o is the maximum current through the diode, R_s is the series resistance, U is the output voltage, q is the electron charge, n is the ideality factor, k is the Boltzmann constant, and T is the temperature.

Formula 2 represents the complete current equation of the solar cell during the circuit connection process [27]. By applying boundary conditions to this equation, modifications are introduced. For this purpose, the parameters at the maximum power point from the current–voltage characteristic graph are used. To determine the maximum power point, it is sufficient to take the product of the maximum current and voltage [28]. Fig. 2 shows the *I–V* characteristic of the solar cell.

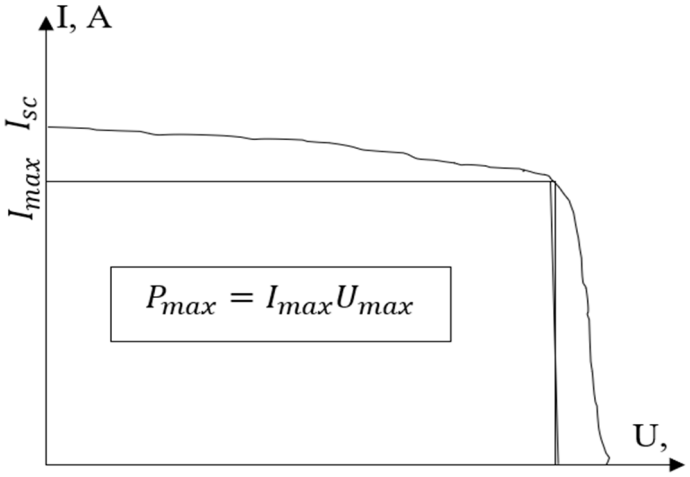

Figure 2. Current–voltage (*I-V)* characteristic of the solar cell.

By determining the *I-V* characteristic of the solar cell, the short-circuit current and open-circuit voltage can be identified. If the initial conditions are set, when the short-circuit current in the *I-V* characteristic approaches zero, the open-circuit voltage takes its maximum value. This can be seen below.

$$U = U_{oc};\ I = I_{sc} = 0. \tag{3}$$

Through the condition in this 3rd formula, we obtain the following equation.

$$I_{ph} = 0 + I_o\left[exp\left(\frac{qU_{oc}}{nkT}\right)-1\right]+\frac{U_{oc}}{R_{sh}}, \tag{4}$$

$$I_{ph} = I_o\left[exp\left(\frac{qU_{oc}}{nkT}\right)-1\right]+\frac{U_{oc}}{R_{sh}}. \tag{5}$$

The 5th formula above clearly allows the determination of the photocurrent passing through the solar cell. Based on these formulas, the current–voltage characteristic of the bifacial solar cell with various metal nanoparticles introduced was determined.

RESULTS AND DISCUSSION

Front-side illumination was applied to the bifacial solar cell with various metal nanoparticles introduced. For comparison purposes, the output parameters of the solar cell without nanoparticles were measured (Fig. 3).

As shown in the graph, all metal types yielded high current densities, with the solar cell without nanoparticles showing the lowest. Positive results were obtained for nanoparticles based on all tested materials. Among them, platinum showed the best performance, reaching a current density of 13.8 mA/cm², while silver produced the lowest value of 5.027 mA/cm². Based on these results, it was decided to continue the experiments with platinum.

The output parameters of the solar cell with platinum nanoparticles increased. These output parameters are significantly dependent on the shape and size of the nanoparticles. Therefore, in the experiment, platinum was taken in spherical form. The spherical particle shape is associated with its ability to generate a uniform field and wave propagation around itself. The sphere's radius was increased in steps of 1 nm. As a result, the dependence of current density on particle radius was obtained (Fig. 4). The introduction of an atom or particle into the solar cell changes its current density. At the same time, the open-circuit voltage depends only on the material type and environmental conditions.

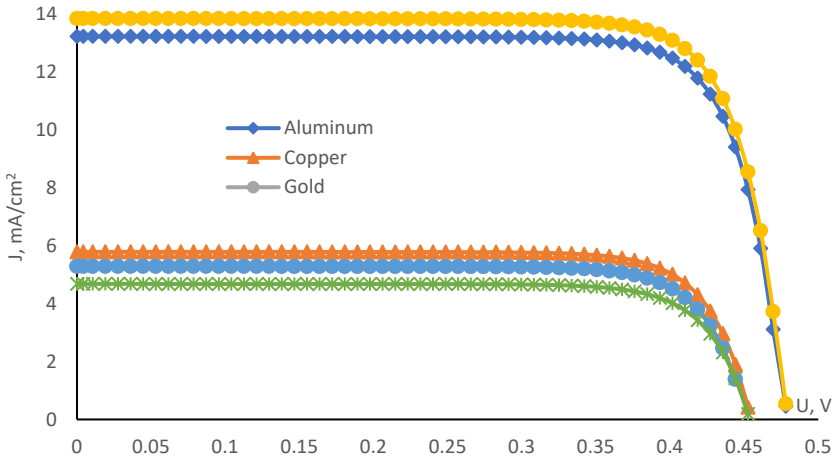

Figure 3. *I–V* characteristics of the bifacial solar cell with various metal nanoparticles

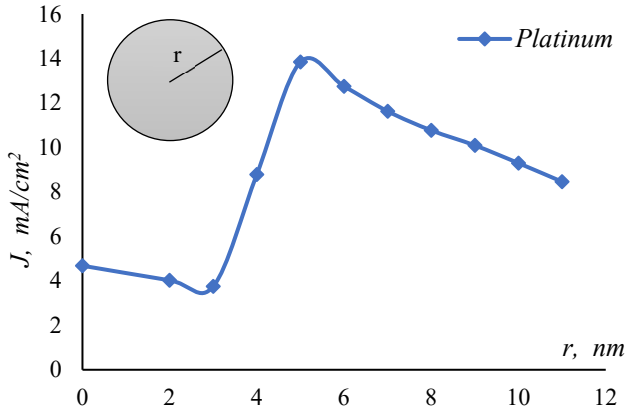

Figure 4. Dependence of the current density of the bifacial solar cell with platinum nanoparticles on the nanoparticle radius.

From the graph in Fig. 4, it can be seen that the current density of the bifacial solar cell with metal nanoparticles shows a significant dependence on the nanoparticle radius. In this case, the nanoparticle size causes the current density to increase in certain ranges and decrease in others. Accordingly, the optimal size of the metal nanoparticle was determined. For platinum nanoparticles, the optimal size was found to be 5 nm. According to the results, the optimal-size current density value was 2.96 times higher than that of the bifacial solar cell without nanoparticles. Measurements also showed that for sizes larger than 5 nm, a decrease in current density was observed. This decrease at sizes larger than the optimal radius is explained by the nanoplasmonic effect occurring in the structure. The occurrence of the nanoplasmonic effect first influences the local electric field, then affects the surface. The spatial extent of the generated electric field should be significantly larger than the nanoparticle size.

Below, the *I–V* and *P–V* characteristics of bifacial solar cells without and with nanoparticles are shown (Fig. 5).

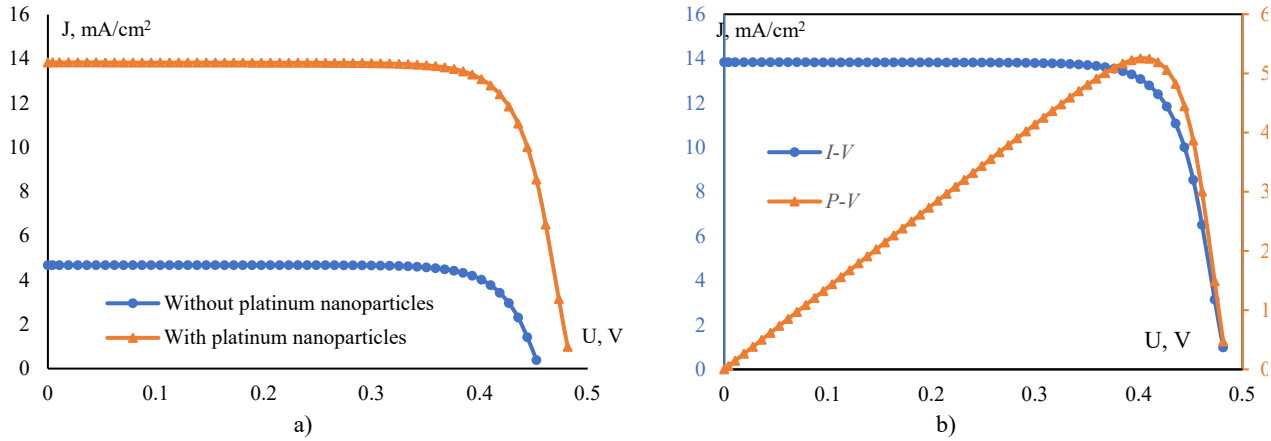

Figure 5. *a) I–V* characteristics of bifacial solar cells with and without platinum nanoparticles, *b) P–V* characteristics of the bifacial solar cell with platinum nanoparticles

From the above graphs, it can be seen that the current density generated by the solar cell with platinum nanoparticles is almost three times higher. Accordingly, the output power and the maximum power point were determined. The

maximum output power was found to be 5.25 mW, with the current density and voltage at this point being 13.08 mA/cm² and 0.401 V, respectively. The relatively small values of the output parameters indicate that the selected sample has a small size. This is because, at smaller sizes, the effect of metal nanoparticles on the selected sample becomes more significant.

The influence of nanoparticles is crucial in achieving higher output parameters. Since the nanoparticles are arranged in a straight line within the emitter layer of the solar cell, an additional light spectrum is generated in that layer. Metals, when exposed to incident light, perform the function of generating charge carriers through the light scattered back from them. The light scattered from the nanoparticles interacts with each other, producing high intensity in that region. As a result, the value of optical generation in that area increases.

The graph of optical generation as a function of solar cell thickness is shown in Fig. 6.

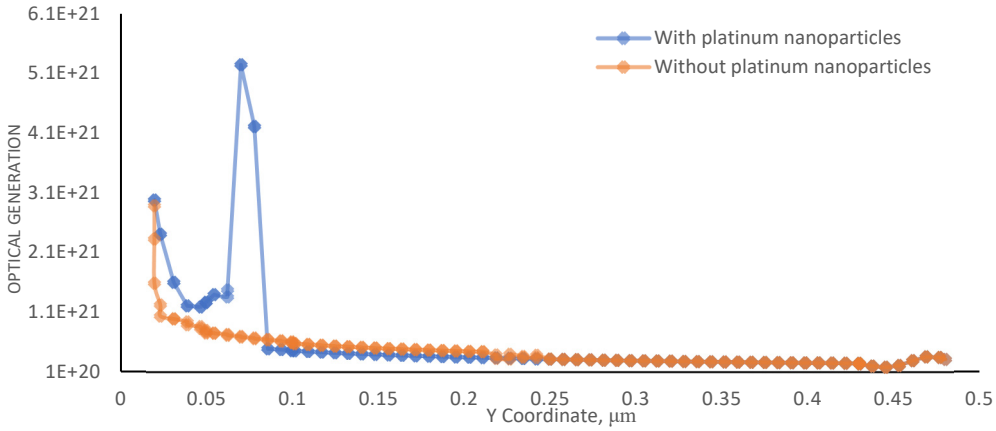

Figure 6. Optical generation of a bifacial solar cell as a function of its thickness

It can be seen from Figure 6 that the nanoparticle embedded in the emitter layer increased the optical generation of the solar cell by almost 1.81 times. In this graph, the optical generation of a solar cell without nanoparticles decreases exponentially. If nanoparticles are not embedded into the emitter layer, light intensity is more absorbed towards the base. Therefore, embedding nanoparticles into the emitter layer increases the light intensity in this layer, resulting in reduced absorption in the base region.

The absorption of light is directly related to its spectrum. Secondly, it is strongly dependent on the thickness of the solar cell. Thickness affects the internal interference process within the solar cell. The optical properties of light in a material are determined by its absorption, transmission, and reflection coefficients. By increasing absorption, it is possible to reduce the values of transmission and reflection coefficients. Therefore, in this research, the dependence of the absorption coefficient on the wavelength of light was determined (Fig. 7).

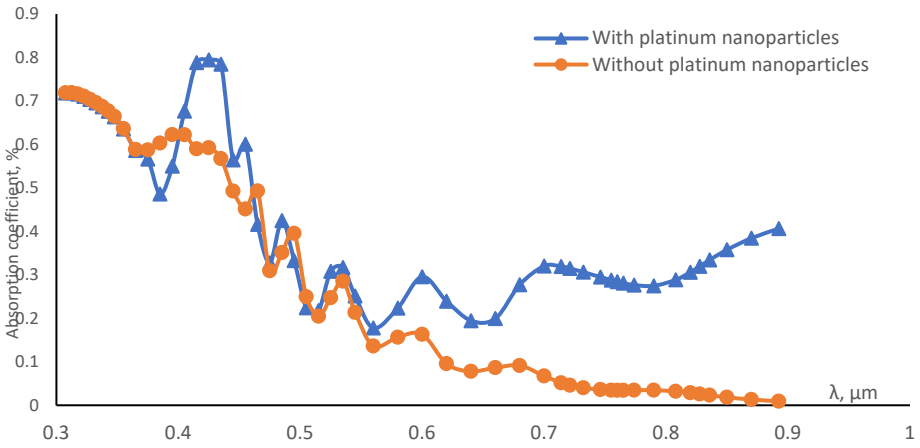

Figure 7. Dependence of the absorption coefficient of a bifacial solar cell on the wavelength of light

The above graph shows that the absorption coefficient of the solar cell with embedded nanoparticles is higher. It was determined that this value is 1.33 times greater than the absorption coefficient of the solar cell without nanoparticles, reaching 79.4%. For the silicon-based bifacial solar cell without nanoparticles, the absorption coefficient decreases as the wavelength of light increases, which leads to inefficient utilization of long-wavelength light. In contrast, the absorption coefficient of the nanoparticle-integrated solar cell shows good performance even at long wavelengths. Based on the obtained results, it can be concluded that the introduction of metal nanoparticles into the bifacial solar cell optimizes its optical properties.

CONCLUSIONS

In this study, various types of metal nanoparticles were introduced into a bifacial solar cell. Among the embedded metal nanoparticles, platinum was identified as the most optimal type. Platinum, a high-efficiency metal, was selected, and its effect on the solar cell's optical properties was investigated. First, the optimal platinum nanoparticle radius for maximum performance was determined. For 5 nm platinum nanoparticles, a current density of 13.8 mA/cm² was achieved. This value was found to be 2.9 times greater than the current density of a solar cell without nanoparticles. Optimal-sized nanoparticles were embedded in the emitter layer of the solar cell, and they were observed to enhance optical generation.

In addition, the absorption coefficient values and corresponding graphs of the nanoparticle-integrated solar cell were obtained. The results showed that absorption increased in the nanoparticle-embedded region and remained effective at long wavelengths. It can be concluded that embedding metal nanoparticles into a bifacial solar cell is a promising approach, as it optimizes its optical properties. In the future, determining the thermal and electrical conductivities of the metal nanoparticles embedded in bifacial solar cells is expected to be even more promising.

Conflict of Interests

The authors declare that they have no conflicts of interest.

Acknowledgments

We would like to express our deepest appreciation to our colleague at the Renewable Energy Source Laboratory at Andijan State University, for their invaluable support throughout this research.

ORCID

Murodjon M. Komilov, https://orcid.org/0009-0006-2080-3371; **Navruzbek A. Mirzaalimov,** https://orcid.org/0000-0002-9264-3710;
Rayimjon Aliev, https://orcid.org/0000-0002-7375-727X; **Avazbek A. Mirzaalimov,** https://orcid.org/0000-0003-2846-1901;
Murodjon K. Abduvohidov, https://orcid.org/0000-0002-7598-8565; **Suhrob R. Aliev** https://orcid.org/0000-0002-4494-8261;
J. Ziyoitdinov, https://orcid.org/0009-0007-6958-4074

REFERENCES

[1] M.A. Green, *Third generation photovoltaics: Advanced solar energy conversion*. Springer Science & Business Media.
[2] A. Cuevas, "The ultimate efficiency of bifacial solar cells," Solar Energy, **112**, 740-745 (2005).
[3] R. Aliev, M. Komilov, N. Mirzaalimov, A. Mirzaalimov, S. Alive, I. Gulomova, and J. Gulomov, "Textured Bifacial Silicon Solar Cells Under Various Illumination Conditions," Journal of Nano and Electronic Physics. **16**(5), 05025-05031 (2024). https://doi.org/10.21272/jnep.16(5).05025
[4] R. Aliev, M. Komilov, S. Aliev, and I. Gulomova, "Comparative analysis of conventional and bifaical solar cells under various illumination conditions," Physics and Chemistry of Solid State, **25**(4), 844–852 (2024). https://doi.org/10.15330/pcss.25.4.844-852
[5] R. Aliev, M. Komilov, I. Gulomova, A. Mirzaalimov, N. Mirzaalimov, S. Aliev, and J. Gulomov, "Effect of temperature on the properties of a bifacial textured solar cell," Vidnovluvana Energetika, **81**(2), 97-105 (2025). https://doi.org/10.36296/1819-8058.2025.2(81).97-105
[6] N.A. Mirzaalimov, R. Aliev, A.A. Mirzaalimov, B.D. Rashidov, S. Qahramonova, and T. Abdulazizov, "Hybrid Solar-Wind Micro-Energy Systems in 3D Format for City Streets," in: *Sustainable Living Solutions: Renewable Energy and Engineering. EDMSET 2024. Advances in Science, Technology & Innovation*, edited by E. Dobjani, *et al.* (Springer, Cham. 2025). https://doi.org/10.1007/978-3-031-76837-8_20
[7] L. Xu, *et al*., "Heat generation and mitigation in silicon solar cells and modules," Joule, **5**(3), 631–645 (2021). https://doi.org/10.1016/J.JOULE.2021.01.012
[8] Y.Q. Gu, C. R. Xue, and M. L. Zheng, "Technologies to Reduce Optical Losses of Silicon Solar Cells," Advanced Materials Research, **953–954**, 91–94 (2014). https://doi.org/10.4028/WWW.SCIENTIFIC.NET/AMR.953-954.91
[9] B. Hoex, M. Dielen, M. Lei, T. Zhang, and C. Y. Lee, "Quantifying optical losses of silicon solar cells with carrier selective hole contacts," AIP Conference Proceedings, **1999**(1), 040010 (2018). https://doi.org/10.1063/1.5049273
[10] B. Kumaragurubaran, and S. Anandhi, "Reduction of reflection losses in solar cell using Anti Reflective coating," in: *2014 International Conference on Computation of Power, Energy, Information and Communication, ICCPEIC*, pp. 155–157, (2014). https://doi.org/10.1109/ICCPEIC.2014.6915357
[11] S.J. Jang, *et al*., "Antireflective property of thin film a-Si solar cell structures with graded refractive index structure," Optics Express, **19**(S2), A108-A117 (2011). https://doi.org/10.1364/OE.19.00A108
[12] S.C. Baker-Finch, and K.R. McIntosh, "Reflection distributions of textured monocrystalline silicon: implications for silicon solar cells," Progress in Photovoltaics: Research and Applications, 21(5), 960–971 (2013). https://doi.org/10.1002/PIP.2186
[13] H. Park, S. Kwon, J.S. Lee, H.J. Lim, S. Yoon, and D. Kim, "Improvement on surface texturing of single crystalline silicon for solar cells by saw-damage etching using an acidic solution," Solar Energy Materials and Solar Cells, 93(10), 1773–1778 (2009). https://doi.org/10.1016/J.SOLMAT.2009.06.012
[14] X. Huang, S. Han, W. Huang, and X. Liu, "Enhancing solar cell efficiency: the search for luminescent materials as spectral converters," Chemical Society Reviews, **42**(1), 173–201 (2012). https://doi.org/10.1039/C2CS35288E
[15] J. Gulomov, and R. Aliev, "The Way of the Increasing Two Times the Efficiency of Silicon Solar Cell," Physics and Chemistry of Solid State, **22**(4), 756–760 (2021). https://doi.org/10.15330/pcss.22.4.756-760.
[16] J. Frank, M. Rüdiger, S. Fischer, J.C. Goldschmidt, and M. Hermle, "Optical Simulation of Bifacial Solar Cells. Energy Procedia,·**27**, 300-305 (2012). https://doi.org/10.1016/j.egypro.2012.07.067
[17] I.A. Yuldoshev, M.Q. Sultonov, and F.M. Yuldashev, *Quyosh energetikasi" darslik*, (Bookany print, Toshkent, 2022).
[18] A. Blakers, N. Zin, K.R. McIntosh, and K. Fong, "High Efficiency Silicon Solar Cells," Energy Procedia, **33**, (2013).

[19] H.A. Atwater, and A. Polman, "Plasmonics for improved photovoltaic devices," Nature materials, **9**(3), 205–213 (2010). https://doi.org/10.1038/nmat2629
[20] M.Z. Nosirov, *et al*., "Photoemission current from metal nanoparticles in silicon," J. Nano- Electron. Phys. **16**(5) 05026 (2024). https://doi.org/10.21272/jnep.16(5).05026
[21] K.R. Catchpole, and A. Polman, "Plasmonic solar cells," Optics Express, **16**(26), 21793–21800 (2008). https://doi.org/10.1364/OE.16.021793
[22] R.A. Pala, J. White, E. Barnard, J. Liu, and M.L. Brongersma, "Design of plasmonic thin-film solar cells with broadband absorption enhancements," Advanced Materials, **21**(34), 3504–3509 (2009). https://doi.org/10.1002/adma.200900331
[23] V.E. Ferry, L.A. Sweatlock, D. Pacifici, and H.A. Atwater, "Plasmonic nanostructure design for efficient light coupling into solar cells," Nano Letters, **8**(12), 4391–4397 (2008). https://doi.org/10.1021/nl8022548
[24] P. Spinelli, M.A. Verschuuren, and A. Polman, "Broadband omnidirectional antireflection coating based on subwavelength surface Mie resonators." Nature Communications, 3, 692 (2012). https://doi.org/10.1038/ncomms1691
[25] J. Zhu, C.M. Hsu, Z. Yu, S. Fan, and Y. Cui, "Nanodome solar cells with efficient light management and self-cleaning," Nano Letters, **10**(6), 1979–1984 (2009). https://doi.org/10.1021/nl9034237
[26] S.L. Khrypko, and G.K. Zholudev, "Modeling of the Electric Characteristics of Photovoltaic Cell Based on Silicon," J. Nano-Electron. Phys. **3**(3), 90-99 (2011).
[27] A.M. Laoufi, B. Dennai, O. Kadi, and M. Fillali, "Study of the Effect of Absorber Layer Thickness of CIGS Solar Cells with Different Band Gap Using SILVACO TCAD," Journal of nano- and electronic physics, **13**(4), 04018 (2021). https://doi.org/10.21272/jnep.13(4).04018
[28] R.V. Zaitsev, and M.V. Kirichenko. Improving the Physical Model of GaAs Solar Cells. Journal of Nano- And Electronic Physics **12**(6), 06015 (2020). https://doi.org/10.21272/jnep.12(6).06015

ПОКРАЩЕННЯ ТА ОПТИМІЗАЦІЯ ОПТИЧНИХ ВЛАСТИВОСТЕЙ ДВУХФАЦІАЛЬНИХ СОНЯЧНИХ ЕЛЕМЕНТІВ ШЛЯХОМ ДОДАННЯ МЕТАЛЕВИХ НАНОЧАСТИНОК

Муроджон М. Комілов[1], Райімжон Алієв[1], Авазбек А. Мірзаалімов[2], С.Р. Алієв[4], Муроджон К. Абдувохідов[3], Наврузбек А. Мірзаалімов[1], Дж. Зійотдінов[1], Содікджон І. Теміров[1]

[1]Андижанський державний університет імені З.М. Бабура, Андижан, Узбекистан
[2]Андижанський державний педагогічний інститут, Андижан, Узбекистан
[3]Андижанська філія Кокандського університету, Андижан, Узбекистан
[4]Андижанський державний технічний інститут, Андижан, Узбекистан

У цьому дослідженні було досліджено зміни оптичних властивостей двостороннього сонячного елемента на основі кремнію зі структурою n^+–p–p^+ за допомогою числового моделювання з використанням програмного середовища Sentaurus TCAD. Різні металеві наночастинки були вбудовані в шар емітера в лінійній конфігурації для аналізу їхнього впливу на процеси поглинання та розсіювання світла. У дослідженні порівнювалися металеві наночастинки платини (Pt), золота (Au), срібла (Ag), алюмінію (Al) та міді (Cu). Всі наночастинки були змодельовані з однаковим діаметром (5 нм), і для кожної конфігурації були отримані вольт-амперні (ВА) характеристики. Результати моделювання показали, що наночастинки платини дали найвищу щільність струму короткого замикання - 13,8 мА/см², тоді як наночастинки срібла дали найнижчу - 5,027 мА/см². Оптимальні параметри спостерігалися для наночастинок діаметром 5 нм. Крім того, було виявлено, що щільність поглинання фотонів для найефективнішого типу металу була в 1,81 рази більшою, ніж у еталонної структури без наночастинок. Крім того, спектральна чутливість кремнію змістилася в ультрафіолетову область у присутності металевих наночастинок. Дослідження продемонструвало покращене використання спектру видимого світла, і завдяки вбудованим наночастинкам загальний коефіцієнт поглинання двостороннього сонячного елемента збільшився в 1,33 рази, що ефективніше узгоджується з видимим спектральним діапазоном.

Ключові слова: *кремній; металеві наночастинки; двосторонній сонячний елемент; TCAD Sentaurus; наноплазмонний ефект*